

## 使用陶瓷基板的寬頻手機天線之研究

# Study of Wideband Handset Antennas on Ceramic Substrates

計畫編號: NSC 89-2213-E-002-104

執行期限: 88 年 8 月 1 日至 89 年 7 月 31 日

計畫主持人: 江蘭富 台灣大學電信研究所

中文摘要 ( 關鍵詞: 陶瓷基板、縮小化天線、積分方程、矩量法。 )

本計畫採用等效電流的觀念及頻域矩量法, 以求解陶瓷基板上縮小化天線的輻射特性。這種方法兼具部分空域矩量法的彈性而又可涵蓋多層介質的效應。此法比模態匹配法更有彈性, 而計算時間也較差分時域法經濟。電流的分佈可由積分方程式求解, 再據此推算輸入阻抗、散射參數、輻射場型等特性。

Abstract ( Key words: ceramic substrate, miniaturized antenna, integral equation, method of moments. )

In this project, the concept of equivalent volume current and method of moments are applied to study the radiation characteristics of miniaturized antennas on ceramic substrates. This approach has the flexibility of spatial domain method of moments and incorporates the effects of layered medium. It is more flexible than the conventional mode-matching technique, and takes less computation time than the FDTD method. The current distribution is obtained by solving the integral equation. Then, the radiation characteristics such as input impedance, scattering parameters, and radiation patterns can be derived from the current distribution.

## 1 Introduction

Materials with high dielectric constant become more important recently due to their capability to reduce the physical size of microwave components in applications like wireless communications. In [1], a modified transmission line model

is proposed to study cavity-backed microstrip antennas. The antenna arrays are placed on thick substrate with high dielectric constant to reduce its dimension. In [2], a portable medium-gain active array antenna consisting of active microstrip antennas is implemented on a ceramic substrate of high dielectric constant for mobile satellite communications.

In [3], the broadside fundamental  $TM_{101}$  mode of an aperture-coupled circular dielectric resonator(DR) antenna using very high dielectric constant is studied. In [4], a small integrated microwave multi-chip modules(MCMs) using high dielectric constant ( $\epsilon_r = 110$ ) substrate is proposed for applications in electronic toll collection. In [5], substrate perforation exterior to a patch antenna is suggested to lower the effective dielectric constant of the surrounding substrate. The surface wave leakage can thus be reduced without affecting the desired radiation characteristics.

In this work, we study the radiation characteristics of patch antennas printed on a substrate with high dielectric constant. Since surface waves might be excited to reduce the radiation efficiency, we first use an artificial waveguide to enclose the substrate so that no surface wave leakage can occur. The size of the waveguide is large enough so that the radiation can be "guided" along the waveguide. The current distribution on the patch surface is then used to calculate the radiation pattern in the absence of the artificial waveguide.

## 2 Solution Procedure

Figure 1 shows a patch antenna printed on a substrate which is enclosed in a rectangular waveguide. The waveguide is used to confine any surface wave modes that might be excited and guided in the substrate which has the form of a dielectric slab waveguide. The problem is thus modeled as a patch antenna embedded in a layered medium enclosed by a rectangular waveguide. The patch is located at the bottom of layer ( $M$ ). The field potential in each layer can be expressed as

$$\begin{aligned}\psi_\ell(\bar{r}) &= \sum_{n=1}^{\infty} \sum_{m=1}^{\infty} \sin\left(\frac{n\pi}{a}x\right) \sin\left(\frac{m\pi}{b}y\right) \\ &\quad \left[ e_{\ell nm}^U e^{ik_{\ell znm}z_\ell} + e_{\ell nm}^D e^{-ik_{\ell znm}z_\ell} \right] \\ \psi'_\ell(\bar{r}) &= \sum_{n=0'}^{\infty} \sum_{m=0'}^{\infty} \cos\left(\frac{n\pi}{a}x\right) \cos\left(\frac{m\pi}{b}y\right) \\ &\quad \left[ h_{\ell nm}^U e^{ik_{\ell znm}z_\ell} + h_{\ell nm}^D e^{-ik_{\ell znm}z_\ell} \right] \\ &\quad 1 \leq \ell \leq N\end{aligned}\quad (1)$$

where  $\psi_\ell(\bar{r})$  and  $\psi'_\ell(\bar{r})$  are the potentials of the  $TM_z$  and  $TE_z$  mode, respectively, in layer ( $\ell$ ),  $z_\ell = z + d_\ell$  with  $1 \leq \ell \leq N$ ,  $k_{\ell znm} = \sqrt{k_\ell^2 - (n\pi/a)^2 - (m\pi/b)^2}$ . The prime on zeros means that the  $n^2 + m^2 = 0$  term is excluded. Next, the tangential electric and magnetic fields in layer ( $\ell$ ) can be derived. The Debye's potential and tangential electric and magnetic fields in layers (0) and ( $t$ ) can be obtained in a similar way.

By imposing the continuity of tangential electric and magnetic fields at interfaces between neighboring layers, four recursive relations for the reflection coefficients are obtained.

At  $z = -d_M$ , impose the conditions that the tangential electric fields are continuous, and the electric surface currents on the patch accounts for the discontinuity of the tangential magnetic fields. Hence, the tangential electric fields at  $z = -d_M$  can be expressed in terms of the Fourier coefficients of the electric surface currents. Impose the final boundary condition that the tangential electric field on the patch is equal

to the impressed field to obtain a set of integral equations.

Next, apply method of moments to solve the integral equations for the current distributions. A set of basis functions are chosen to expand the electric surface currents. The same set of basis functions are also used as weighting functions. Then, take the inner product of these weighting functions with the integral equations to obtain a matrix equation.

In order to calculate the radiation field, the waveguide is removed, and each layer is extended to infinity horizontally. The Debye's potentials, tangential electric and magnetic fields in this open structure can be derived in a similar manner.

Next, the same sets of basis functions as used in the closed structure are used to expand the surface currents. The expansion coefficients  $\{u_p\}$  and  $\{v_p\}$  are obtained by solving (??). The  $z$ -component of the fields in layer(0) can be expressed as a function of the surface currents. The radiation(far) field is then calculated by applying the stationary phase approximation. Thus, we have

$$\begin{aligned}E_{0z}(\bar{r}) &= \frac{e^{ik_0 r}}{r} 2\pi\eta_0 k_0 \cos\theta \\ &\quad \left[ -\sin\theta \cos\phi \tilde{K}_x(\bar{k}_s) - \sin\theta \sin\phi \tilde{K}_y(\bar{k}_s) \right] \\ &\quad \left[ 1 - \frac{R_{12}^{TM} e^{2ik_{1z}h_1} + 1}{R_{12}^{TM} e^{2ik_{1z}h_1} - 1} \epsilon_1 k_{0z} \right]^{-1} \\ H_{0z}(\bar{r}) &= \frac{e^{ik_0 r}}{r} 2\pi \frac{k_0}{\eta_0} \cos\theta \\ &\quad \left[ -\sin\theta \sin\phi \tilde{K}_x(\bar{k}_s) + \sin\theta \cos\phi \tilde{K}_y(\bar{k}_s) \right] \\ &\quad \left[ \frac{k_{0z}}{\omega\mu_0} - \frac{k_{1z}}{\omega\mu_0} \frac{R_{12}^{TE} e^{2ik_{1z}h_1} - 1}{R_{12}^{TE} e^{2ik_{1z}h_1} + 1} \right]^{-1}\end{aligned}\quad (2)$$

where  $k_x = k_0 \sin\theta \cos\phi$ ,  $k_y = k_0 \sin\theta \sin\phi$ , and  $\eta_0$  is the intrinsic impedance in layer(0). The tangential field components are then derived as

$$E_{0\theta}(\bar{r}) = -\frac{E_{0z}(\bar{r})}{\sin\theta}, \quad E_{0\phi}(\bar{r}) = \eta_0 \frac{H_{0z}(\bar{r})}{\sin\theta}$$

### 3 Results and Discussions

Figure 2 shows the input impedance of a patch antenna on a substrate backed by copper. The patch and substrate are enclosed by a rectangular waveguide with the cross section of 4 m by 4 m. The cross section is wide enough that the frequencies considered are higher than the cutoff frequency of the dominant mode of the waveguide. The waveguide serves the purpose of confining the surface wave modes which can cause leakage. The impedance shows a resonance near  $f = 280$  MHz, and the bandwidth is quite narrow as in conventional microstrip antennas.

Figure 3 shows the distribution of  $E_z$  amplitude underneath the patch. The fields mainly concentrate underneath the patch, and become vanishingly small away from the patch.

Figure 4 shows the phase distribution associated with Figure 3. The phase over the left half remains about the same, and the phase over the right half is  $180^\circ$  out of phase. Phase varies rapidly near the center line of the patch and around the perimeter of the patch.

The amplitude and phase informations are combined to give the real and imaginary part of the  $E_z$  component. The real part is much larger than the imaginary part, indicating that the  $E_z$  field component is in phase with the driving voltage source.

Consider a rectangular cavity where the top and bottom surfaces are perfect electric conductors, and the four side surfaces are perfect magnetic conductors. The resonant frequencies of the eigen modes in such a cavity are  $[(m\pi/a)^2 + (n\pi/b)^2 + (p\pi/d)^2]^{1/2}/2\pi\sqrt{\mu_o\epsilon_1\epsilon_o}$  where  $a, b$  are the widths of the top surface, and  $d$  is the distance between the top and bottom surfaces. The resonant frequency of the  $TM_{100}$  mode is 300 MHz.

Compared with the  $E_z$  components of the cavity model, it is observed that the edge effect along the edges at  $y = c_y \pm w_y/2$  is much stronger than that in Figures 3 and 4. The strong field near the driving stub also contributes to the deviation of the resonant frequencies.

### 4 Conclusions

A layered-medium formulation is proposed to study the radiation characteristics of a patch antenna on a substrate with high dielectric constant. An artificial rectangular waveguide is used to eliminate the effect of surface wave leakage. The current distribution is then used to calculate the radiation field by using stationary phase approximation. Input impedance and field distributions are presented to discuss the major mechanism of radiation.

### References

- [1] S. M. Duffy and M. A. Gouker, "A modified transmission line model for cavity-backed microstrip antennas," *IEEE AP-S Intl. Symp.*, vol.4, pp.2139-2142, July 1997.
- [2] R. Miura, R. Suzuki, N. Hamamoto, and Y. Matsumoto, "Active array antenna with ceramic substrate for TDM/TDMA mobile satellite communications," *IEEE GLOBE-COM'93.*, vol.1, pp.564-568, Nov.29-Dec.2, 1993.
- [3] K. W. Leung and K. M. Luk, "Circular dielectric resonator antenna of high dielectric constant for low-profile applications," *IEEE 9th Intl. Conf. Antennas Propagat.*, vol.1, pp.517-519, 1995.
- [4] M. Murase, Y. Sasaki, A. Sasabata, H. Tanaka, and Y. Ishikawa, "Multi-chip transmitter/receiver module using high dielectric substrates for 5.8 GHz ITS applications," *IEEE MTT-S Intl. Microwave Symp.*, vol.1, pp.211-214, June 1999.
- [5] J. S. Colburn and Y. Rahmat-Samii, "Patch antennas on externally perforated high dielectric constant substrates," *IEEE Trans. Antennas Propagat.*, vol.47, pp.1785-1794, Dec. 1999.

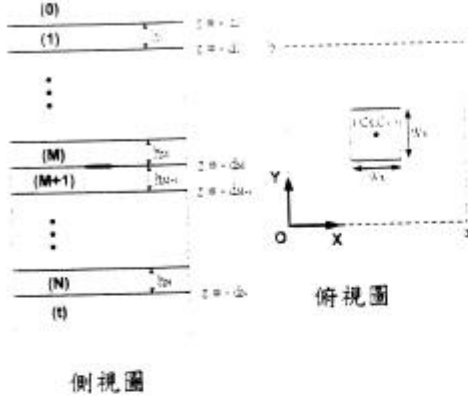


Figure 1: Configuration of a patch antenna enclosed by a rectangular waveguide.

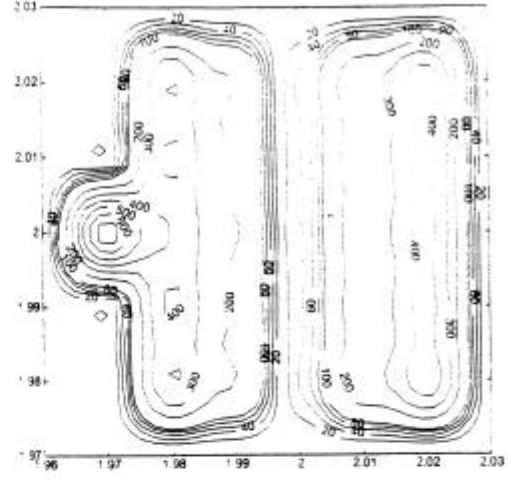


Figure 3: Distribution of  $E_z$  amplitude underneath the patch, parameters the same as in Fig.2.  $z = -d_0 - h_1/2$ .  $f = 280.5$  MHz.

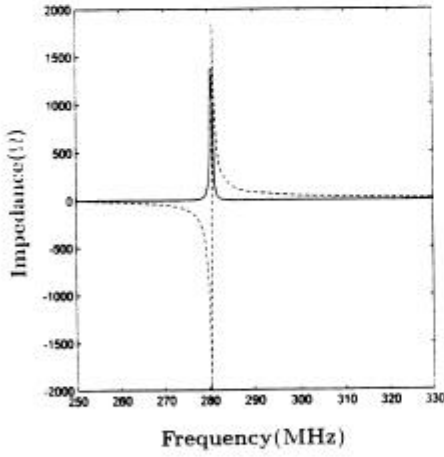


Figure 2: Input impedance of a patch antenna in a three-layered medium enclosed by a rectangular waveguide,  $M = 0$ ,  $N = 1$ ,  $t = 2$ ,  $h_1 = 2$  mm,  $\epsilon_0 = \epsilon_o$ ,  $\epsilon_1 = 100\epsilon_o$ ,  $\epsilon_2 = \epsilon_o$ ,  $\sigma_2 = 5.92 \times 10^7$  S/m,  $a = 4$  m,  $b = 4$  m,  $c_x = 2$  m,  $c_y = 2$  m,  $w_x = 5$  cm,  $w_y = 5$  cm.

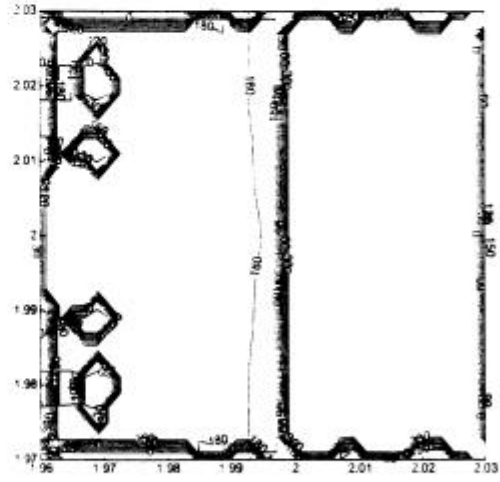


Figure 4: Distribution of  $E_z$  phase underneath the patch, parameters the same as in Fig.2.  $z = -d_0 - h_1/2$ .  $f = 280.5$  MHz.